МАТЕМАТИЧЕСКОЕ МОДЕЛИРОВАНИЕ, ЧИСЛЕННЫЕ МЕТОДЫ И КОМПЛЕКСЫ ПРОГРАММ/MATHEMATICAL MODELING, NUMERICAL METHODS AND PROGRAM COMPLEXES

DOI: https://doi.org/10.60797/COMP.2026.9.2

A METHODOLOGY REVIEW FOR WAVE-ATTRACTOR PROBLEMS

Research article

Elistratov S.A.[1,] *

[1] ORCID : 0000-0002-7006-6879;

[1] Ivannikov Institute for System Programming of RAS, Moscow, Russian Federation

[1] Shirshov Institute of Oceanology of Russian Academy of Sciences, Moscow, Russian Federation

* Corresponding author (sa.elist-ratov[at]yandex.ru)

Abstract

Wave attractors are specific and complex flows, formed by a self-focused internal or inertial waves. In linear regimes they appear as clear coherent structures of a certain shape; in non-linear ones the intensive formation of the secondary waves occurs which distort the coherent structure. Their presence, along with the huge localization of the flow, makes one to select thoroughly the post-processing methods in such flows (including energy characteristic calculation, spectral investigation, visualization etc.). In the existing articles, these methods vary from work to work. The goal of this paper is to consider different method for processing the flow data applied to wave attractors in order to compare their particularities and to reveal the best practice for the further using.

Keywords: wave attractors, methodology, applied math.

ОБЗОР МЕТОДОВ АНАЛИЗА ЗАДАЧ С ВОЛНОВЫМИ АТТРАКТОРАМИ

Научная статья

Елистратов С.А.[1,] *

[1] ORCID : 0000-0002-7006-6879;

[1] Институт системного программирования им. В. П. Иванникова, Москва, Российская Федерация

[1] Институт океанологии им. П.П.Ширшова РАН, Москва, Российская Федерация

* Корреспондирующий автор (sa.elist-ratov[at]yandex.ru)

Аннотация

Волновые аттракторы представляют собой специфические течения со сложной структурой, сформированные в результате самофокусировки внутренних или инерционных волн. В линейных режимах они представляют собой когерентную структуру определенной формы; в нелинейных происходит интенсивное образование вторичных волн, которые искажают эту структуру. Их наличие наряду с сильной локализацией течения заставляет тщательно подходить к выбору методов обработки для такого рода течений (включая вычисление энергетических характеристик, спектральных методов и т.д.). В существующих работах эти методы различаются в зависимости от конкретной статьи. Целью настоящего исследования является рассмотрение различных методов обработки данных течений применительно к волновым аттракторам с целью сравнения их особенностей и определения наилучших для дальнейшего использования.

Ключевые слова: волновые аттракторы, методология, численные методы.

Introduction

A wave attractor is a result of internal/inertial waves self focusing [1]. The main feature of the wave attractor is the huge ratio between the amplitude on it and that of the wave-maker [2], [3], which causes the wave instability at the respectively small wave-maker amplitudes [4]. Such flows are characterized by the great energy accumulation and specific spectrum caused by the wave instability appeared in these flows [5] which are frequently calculated and investigate qualitatively as well as quantitatively, which means they should be, on the one hand, precise enough to reflex the complex structure of the flow, and on the other hand, be general-purpose to require minimal setup and to have clear requirements to be applied (such as signal point number etc.). However, there appear to be the variety of methods, changing from work to work, that requires the thorough investigation and comparison of these technical methods themselves.

In this investigation, the corresponding review of the methods used for wave-attractors flow processing will be conducted. For this purpose, the numerical simulation result will be used following [2], [6], [7], [10]; 2D formulation, whose accuracy is shown in [2], [7], [9], [11], is applied to save computational resources.

Research methods and principles

The simulation is conducted in open-source package *Nek5000* [12], using spectral-element approach for high-order simulation, which is validated for wave-attractor flow simulation [10], [13], [14], [15]. For the internal waves propagation, the stratification is required which is created by dissolved salt stratification in water. The following system of equations is solved:

$$\frac{\partial \vec{v}}{\partial t} + \left(\vec{v}, \nabla\right) \vec{v} = -\frac{1}{\rho_m} \nabla \tilde{p} + \frac{\rho_s}{\rho_m} \vec{g} + \nu \Delta \vec{v} \quad (1)$$

$$\frac{\partial \rho_s}{\partial t} + \left(\vec{v}, \nabla\right) \rho_s = \lambda_s \Delta \rho_s \tag{2}$$

$$\operatorname{div} \vec{v} = 0 \tag{3}$$

These are Navier-Stokes equation in Boussinesq approximation, dissolved salt transport and continuity equation. Here $\tilde{p}$ denotes the pressure excluding the hydrostatic part $g\rho_m$, (g is the gravity acceleration modulus), $\rho = \rho_m + \rho_s$ is the full density consisted of ρ_m (fresh water density) and ρ_s (the solution density increases due to salt admixture); λ_s is the salt diffusivity coefficient. During the simulation, Schmidt number $Sch = \nu/\lambda_s = 700$.

For the focusing, internal waves require a slope [1]; thus, the minimal geometry for wave attractors study is a trapezium, as shown on Fig.1. This study will mainly use the trapezium-shaped domain except the case with mid-depth plateau, whose geometry will be shown in what follows.

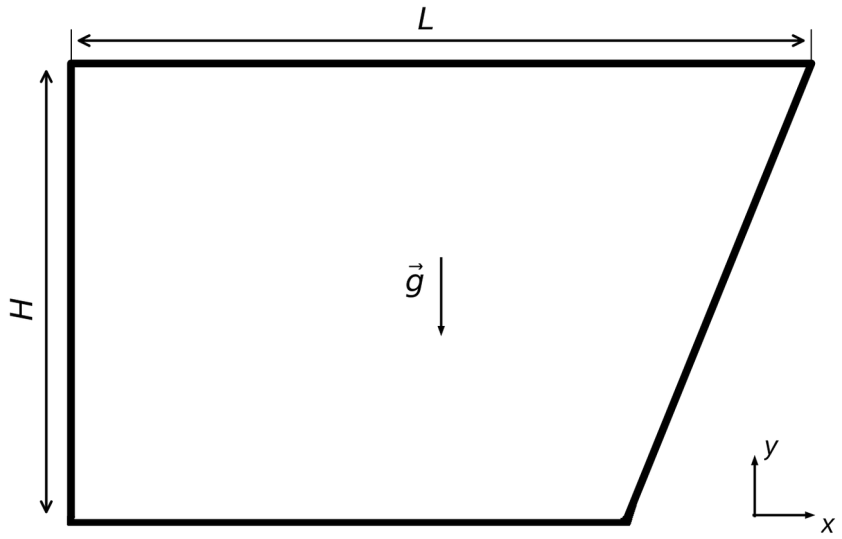

Figure 1 - Domain principle outline
DOI: https://doi.org/10.60797/COMP.2026.9.2.1

To generate internal waves, wave-maker is used in the form of an oscillating boundary [16], [17], [18]. For small oscillation amplitudes $a << H$ it is reasonable to use a velocity condition instead of the moving-shape domain. In what follows, we used wave maker on the upper boundary, with the oscillation dependency $v_y^{wm}(x,t) = a\sin(\omega_0 t)\sin(2\pi x/L)$. Note that its integral is $ which is required to fit the mass conservation law. Here and forward, $T_0 = 2\pi/\omega_0$ is wave-maker period (used for time non-dimensionalization), $f = \omega/(2\pi)$.

The other specific parameters (like viscosity, startification profile, wave-maker amplitude and frequency etc.) are varied from case to case; the specific values can be found in the article describing each particular case (the link will be provided in the corresponding sections).

Main results

3.1. Energy Local Average Calculation

Kinetic energy is one of the most frequently appearing characteristics when discussing wave attractors. Its popularity is based on its huge values typical for this flow type.

The total kinetic energy is defined as

$$E = \frac{\rho_m}{2} \iiint_V \left(v_x^2 + v_y^2\right) dV \tag{4}$$

where V is a domain volume. Even in a linear regime, this value will increase with a wave-maker amplitude a ; thus, it is reasonably to consider the relative kinetic energy [19]:

$$\overline{E} = E/E_w, \quad E_w = \frac{1}{2}\rho_m V (a\omega_0)^2 \tag{5}$$

In wave attractor flows, the $\overline{E} >> 1$ [5], [20], varying from ~ 10 [21] to ~ 1000 [3]. Such huge values are also considered as indirect evidence of a wave-attractor presence. The more the relative kinetic energy, the higher the energy accumulation on the attractor, so the instability will appear at lower wave-maker intensities.

Since both energy and relative energy differ to a constant, their behaviour is the same, and the principles considered in what follows are applicable to both of them to the same extent.

The energy behaves specifically in time: at the formation process it grows, that reach the saturation, after which begins to "noise" (it is conditioned by the additional harmonics from the secondary waves). The energy has a tendency to oscillate even in a linear regime [3], [21], [22] it occurs due to a presence of the standing waves along with the running ones.

To describe the system, the local average value is used (the oscillations are excluded); however, because of the rapid increase at the beginning and non-linear oscillations, the average obtaining becomes a non-trivial problem. Local average is required to maintain the following principle properties: to start from zero (as the real kinetic energy) and to not start to oscillate while the instability develops.

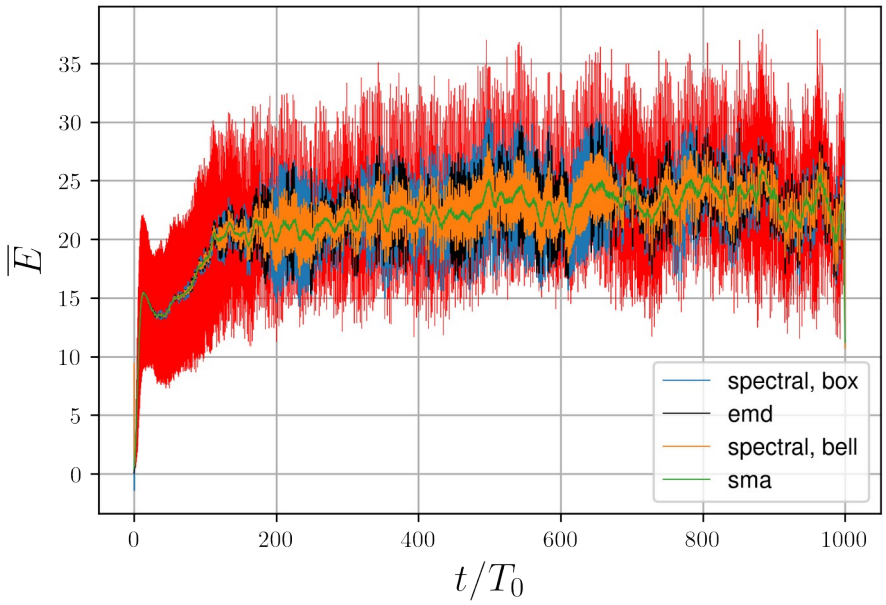

Figure 2 - Energy behaviour in a non-linear regime (red) with different methods of the local average estimation
DOI: https://doi.org/10.60797/COMP.2026.9.2.2

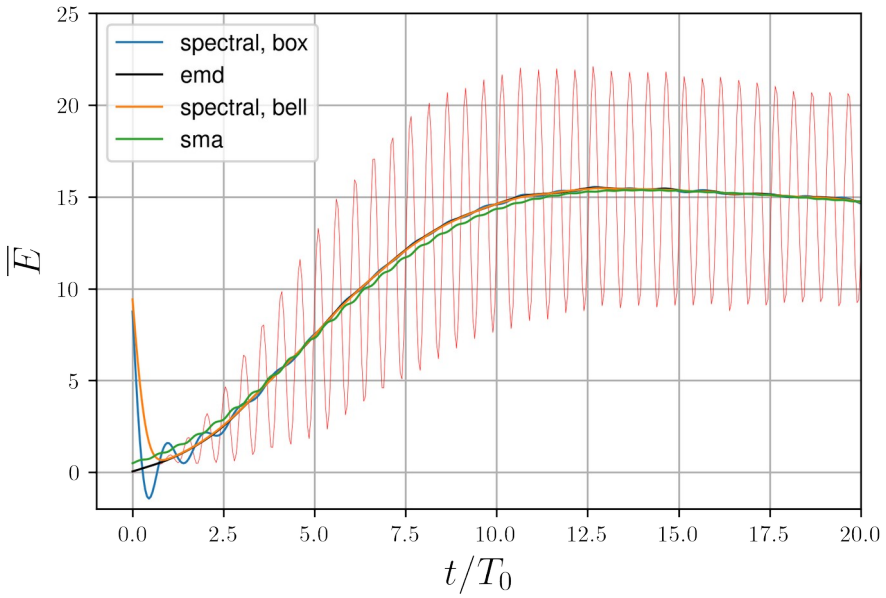

Figure 3 - Energy at the attractor fomation time range
DOI: https://doi.org/10.60797/COMP.2026.9.2.3

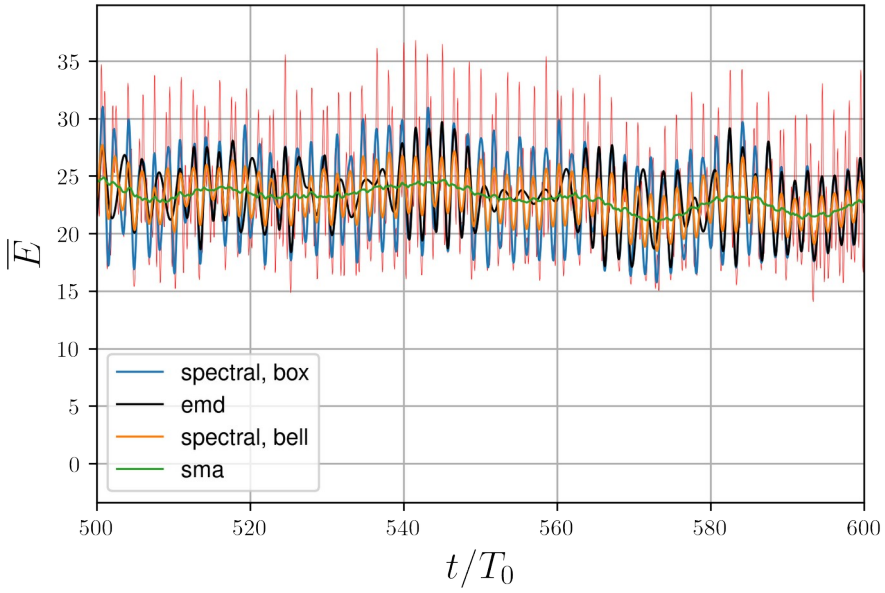

Figure 4 - Energy at the developed instability
DOI: https://doi.org/10.60797/COMP.2026.9.2.4

Fig. 2 considers different methods for local average estimation. One of the popular is EMD-filtration [3], [23], [24]. The signal is decomposed into the automatically-calculated empirical modes, sorted into the frequency-descended order; than the first several (with the highest frequencies) are neglected:

$$\overline{E}_{avg}(t) = \overline{E} - \sum_{i=1}^{N_{EMD}} IMF_i(t) \quad (6)$$

The method does not require special fitting and is governed by the number of filtration modes. The increase of N_{EMD} (making smoother) worsen the start reproducing (near $t/T_0 \to 0$, Fig. 3), and a lack of them leads to oscillations for heavily non-linear cases (black line on Fig. 4). The optimal filtered modes number N_{EMD} for initial range resolution is no more than 2, for instability oscillations smoothing at least 4 is recommended.

The next idea is the spectral filtration; the higher frequencies of the spectrum are suppressed, and then the inverse transform is conducted:

$$\overline{E}_{avg}(t) = FFT^{-1}\left(\hat{w}(f)FFT(\overline{E}(t))\right) \quad (7)$$

The different filter action on a real energy spectrum is represented on Fig. 5; the "box" filter is $\hat{w}(f) = \sigma\left(-(f - f_{thr})\right)$ (σ is Heaviside step function), shown for the threshold frequency $f_{thr} = f_0$, and the "bell" one is the gaussian filter $\hat{w}(f) = \exp\left(-\frac{f^2}{2\hat{\sigma}}\right)$, for bell semiwidth $\hat{\sigma} = f_0$. For both filters, there is the same problem: the narrower filters do not reproduce correctly the initial increase (Fig. 3), the wider ones oscillate at the instability formation times (Fig. 4). For boxcar filter, $f_{thr} < 0.5f_0$ is enough for long-term average, but the growth range will be resolved only at $f_{thr} = 1.5f_0$. For gaussian bell filter type, $\hat{\sigma} = 2f_0$ is suitable, however, non-zero values at $t = 0$ (as shown on Fig. 3) occurs at any $\hat{\sigma}$ because of the peculiarities of the filter shape.

Figure 5 - Energy spectrum with different filtartion
DOI: https://doi.org/10.60797/COMP.2026.9.2.5

The third method is the moving average:

$$\overline{E}_{avg}(t) = \frac{1}{T_w} \int_{t-T_w/2}^{t+T_w/2} \overline{E}(t) w(t) dt \tag{8}$$

where $w(t)$ is a window with support size T_w used to smoothen the curve. This method can seem to underestimate the average on the rapid initial growth; however, the correct window size T_w selection (Fig. 6) allow to achieve the good initial reproduction as well as the oscillation suppression (Fig. 7), with optimal $T_w = 4T_0$. The larger ranges lead to failure at the initial time, the smaller ones tend to oscillate at the instability development times. A specific window type (Hamming, Blackman, etc.) using turns out to make no influence the result (Fig. 8,9).

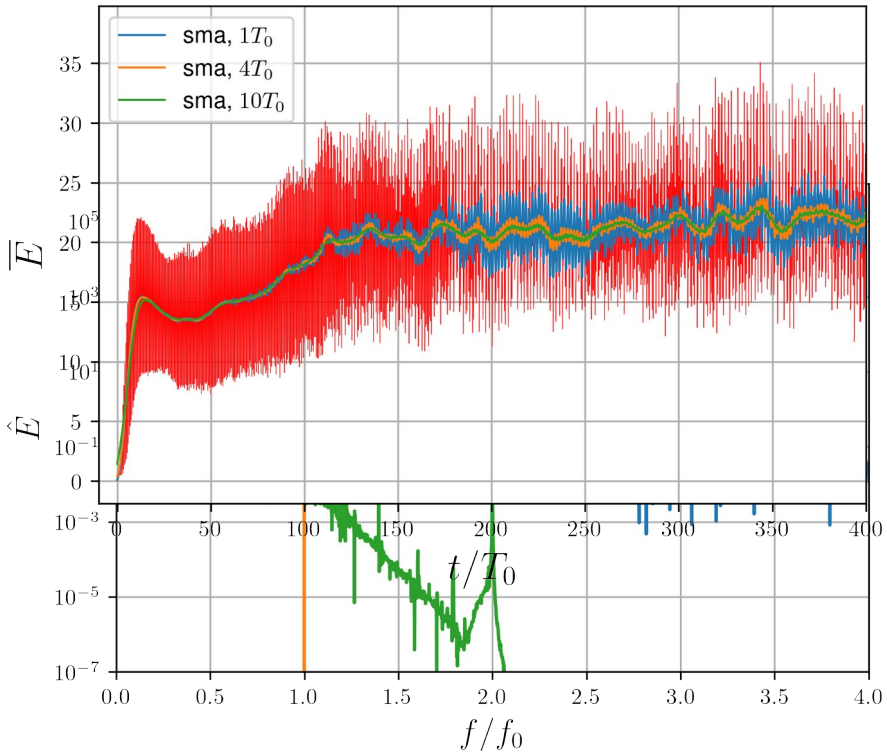

Figure 6 - Energy local average calculation with simple moving average
DOI: https://doi.org/10.60797/COMP.2026.9.2.6

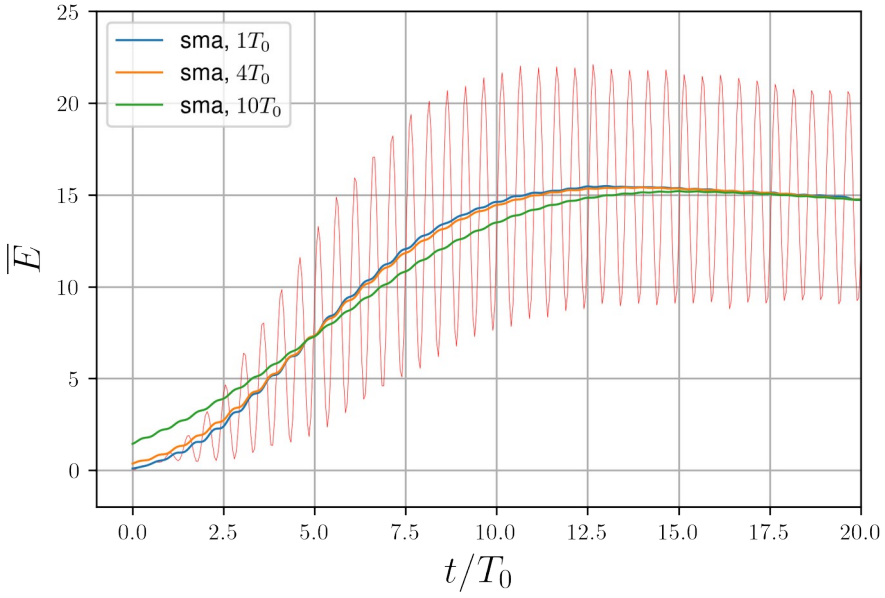

Figure 7 - Moving average action at the attractor formation time: the window width influence
DOI: https://doi.org/10.60797/COMP.2026.9.2.7

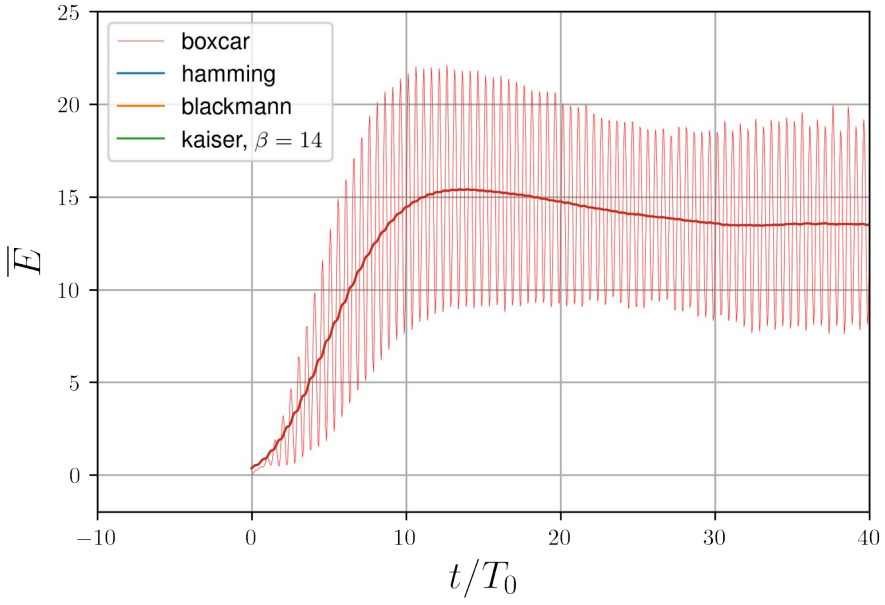

Figure 8 - Window influence on the moving average calculation: formation times
DOI: https://doi.org/10.60797/COMP.2026.9.2.8

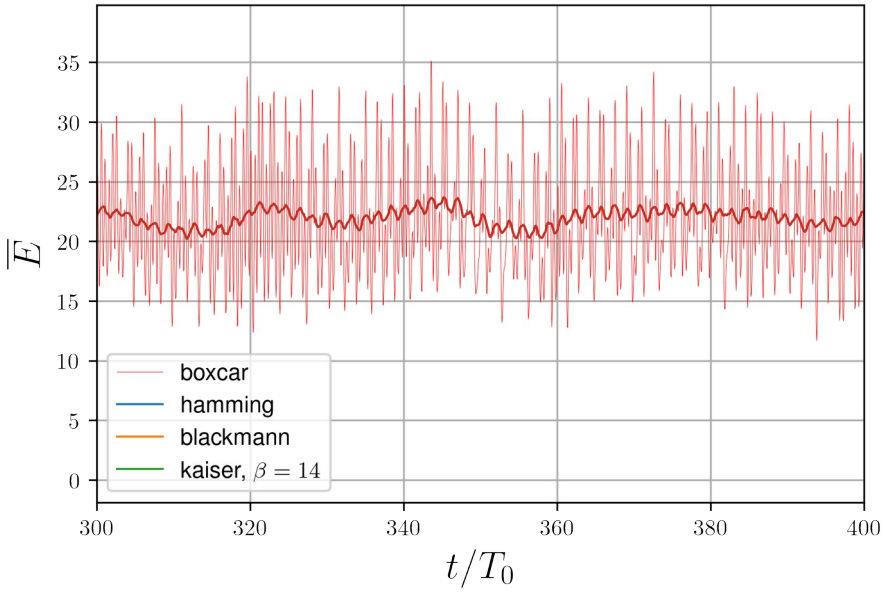

Figure 9 - Moving average calculation: developed instability
DOI: https://doi.org/10.60797/COMP.2026.9.2.9

3.2. Spectrum Position Influence

The temporal spectra, while calculated for an attractor flow, are investigated in a point; as a representative point, the attractor's ray middle (Point 4 on Fig. 10) is usually considered [3], [21], [22], [25].

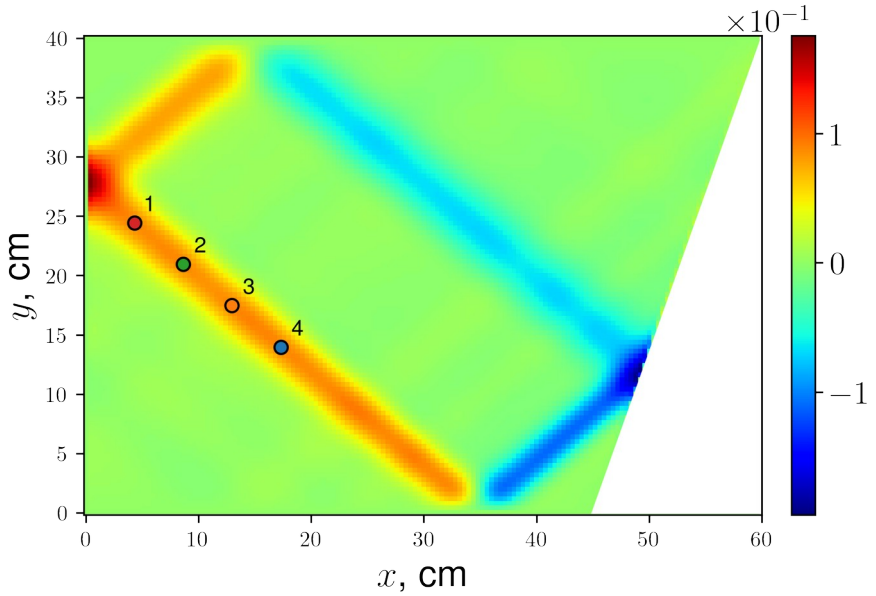

Figure 10 - Liner attractor regime, v_y snapshot and spectrum calculation locations
DOI: https://doi.org/10.60797/COMP.2026.9.2.10

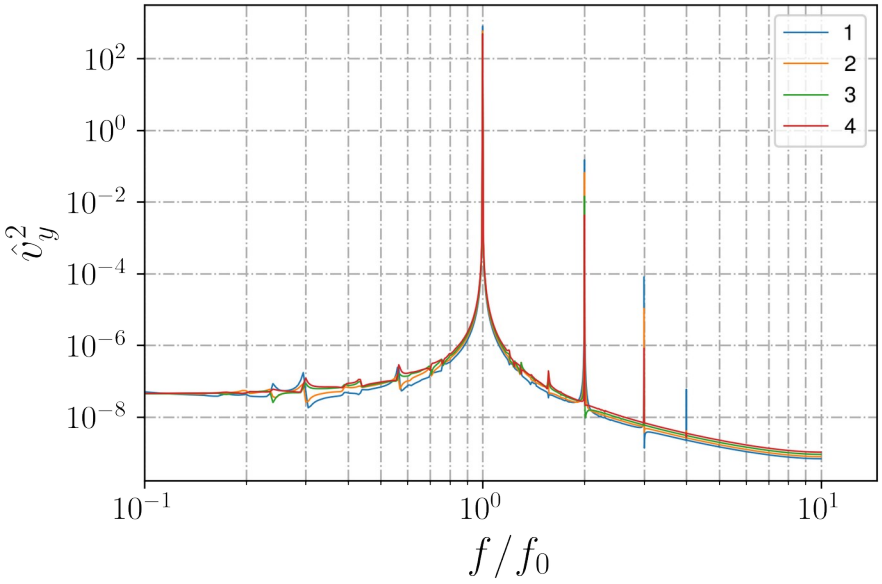

Figure 11 - Linear attractor regime, spectra in different locations
DOI: https://doi.org/10.60797/COMP.2026.9.2.11

The closer investigation shows that there is no principle difference which point on the ray to considered, as shown on Fig. 11; neither it is for an elongated geometry (Fig. 12,13) from [3]. The difference between the spectra calculated does not exceed 11%.

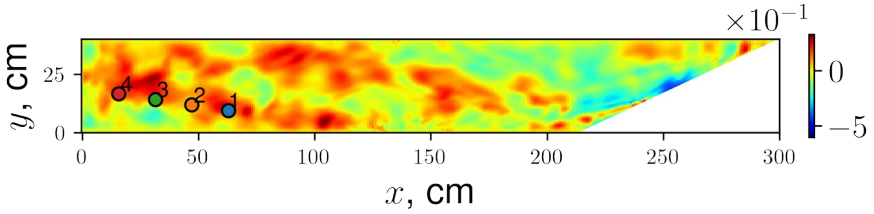

Figure 12 - Non-linear attractor regime in a large-aspect ration domain, v_y snapshot and spectrum calculation locations
DOI: https://doi.org/10.60797/COMP.2026.9.2.12

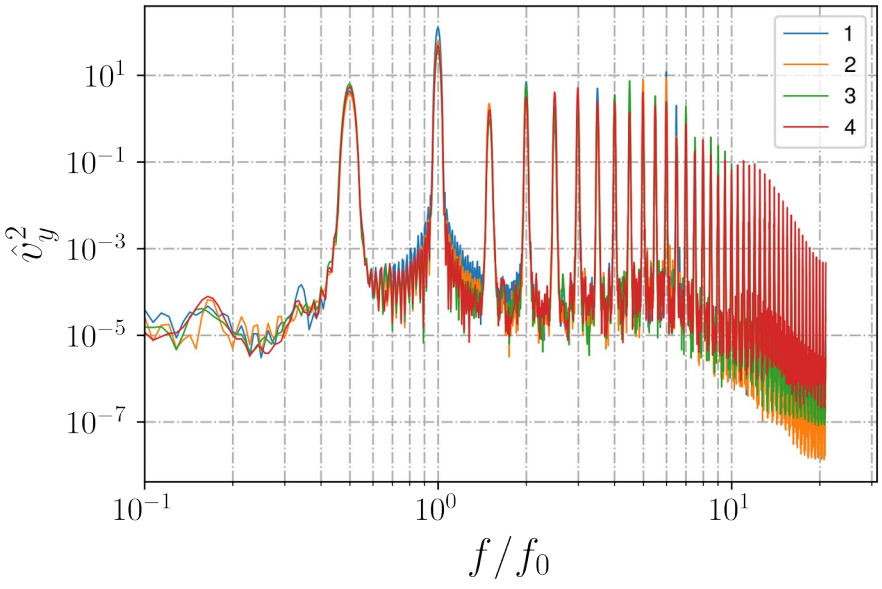

Figure 13 - Spectra in different locations for large-aspect ratio attractor
DOI: https://doi.org/10.60797/COMP.2026.9.2.13

For a limited-depth attractor of (n,1) type from work [26], shown on Fig. 14, it is shown that different attractor cells do not principally differ in spectral terms (Fig. 15), with 6% difference.

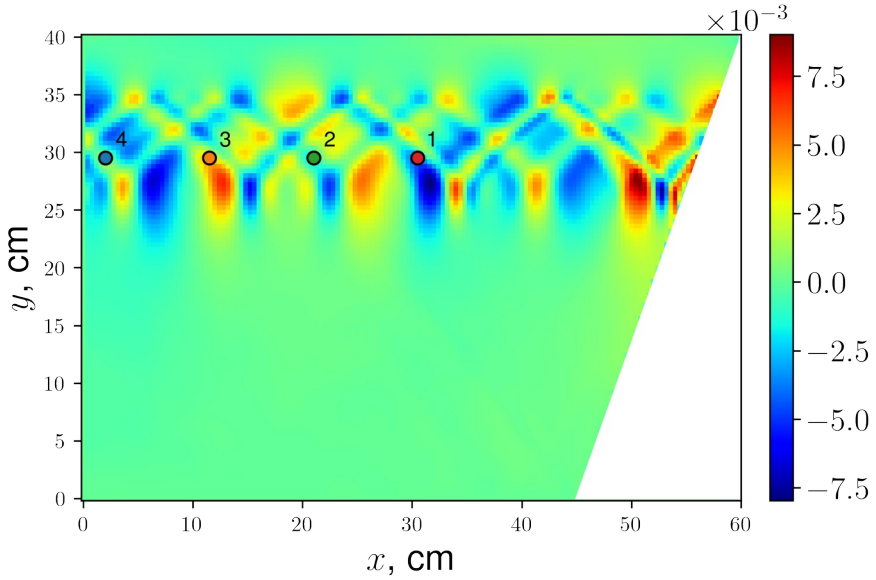

Figure 14 - Attractor in a layer, v_y snapshot and spectrum calculation locations
DOI: https://doi.org/10.60797/COMP.2026.9.2.14

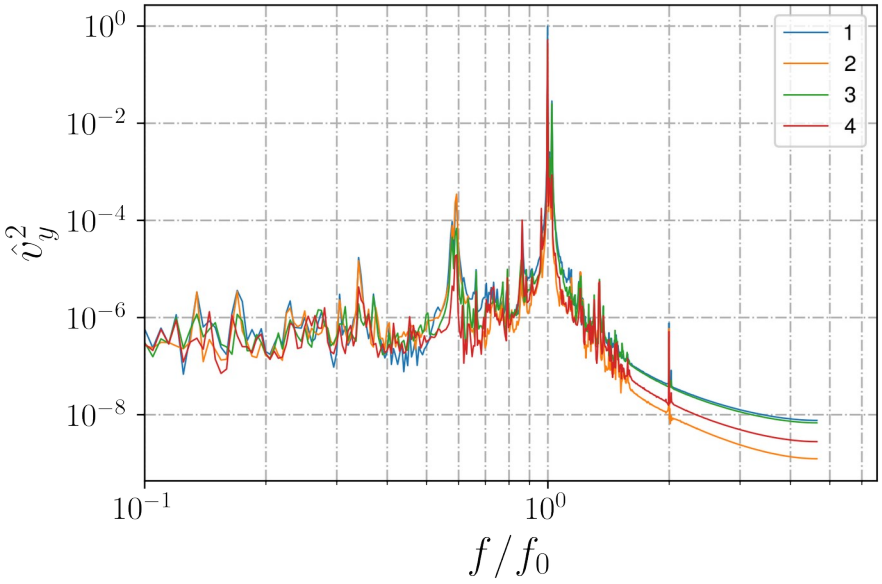

Figure 15 - Attractor in a layer spectra in different locations
DOI: https://doi.org/10.60797/COMP.2026.9.2.15

A bit different situation takes place in case of an attractor with mid-depth peak (Fig. 16,18) from [27]. This attractor differs from the other ones since it has continuous spectrum; the spectra turn out to be more saturated in the points closer to the walls (Fig. 17,19) in a non-linear regime, with the difference between them being up to 43%. However, their qualitative properties remain the same.

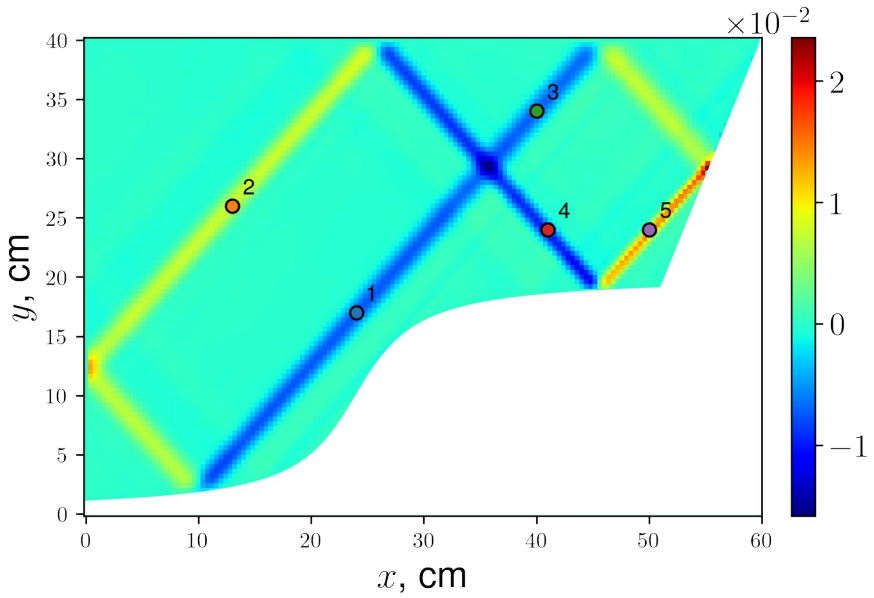

Figure 16 - (2,1) linear-regime attractor in a domain with underwater plateau, v_y snapshot and spectrum calculation locations

DOI: https://doi.org/10.60797/COMP.2026.9.2.16

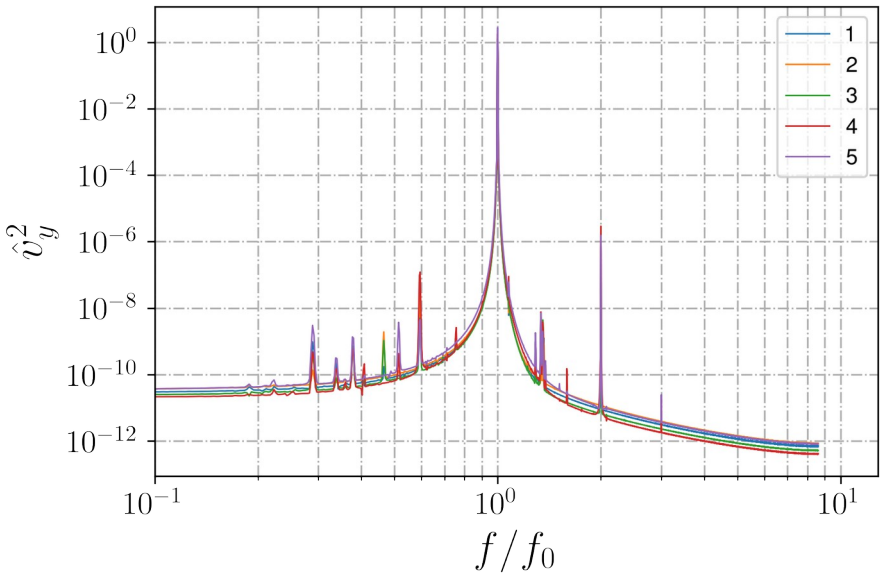

Figure 17 - Spectra in different locations for attractor in basin with underwater plateau, linear regime

DOI: https://doi.org/10.60797/COMP.2026.9.2.17

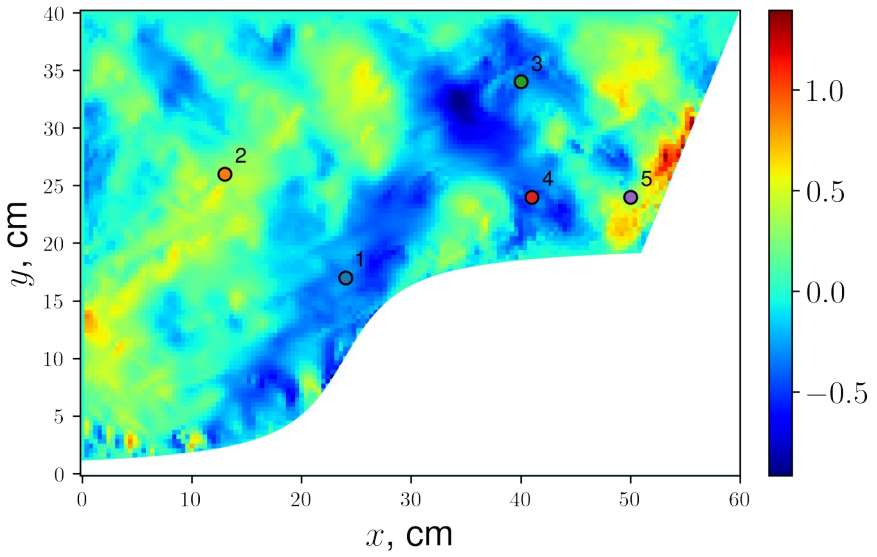

Figure 18 - (2,1) non-linear attractor in a domain with underwater plateau, v_y snapshot and spectrum calculation locations
DOI: https://doi.org/10.60797/COMP.2026.9.2.18

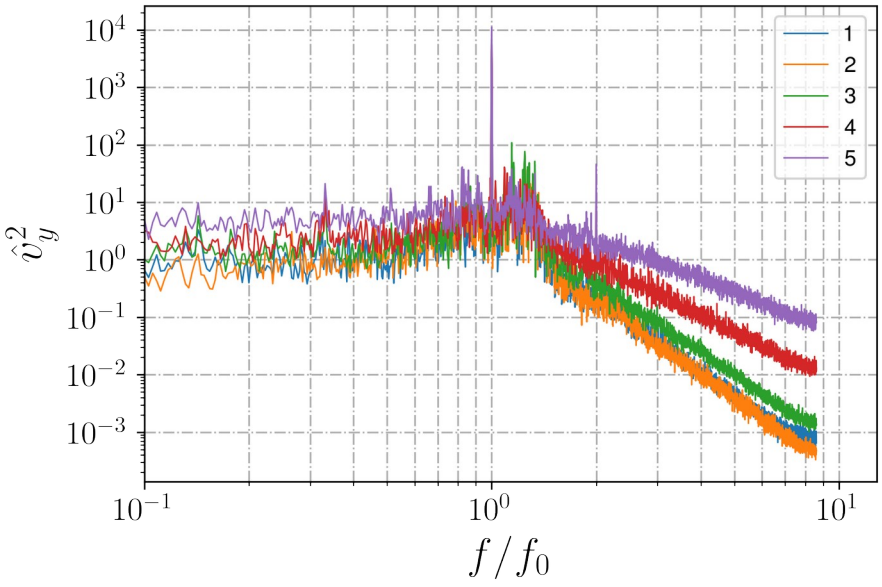

Figure 19 - Spectra in different locations for attractor in basin with underwater plateau, non-linear regime
DOI: https://doi.org/10.60797/COMP.2026.9.2.19

3.3. Spectral Window

To improve the spectrum, windows are often applied. There is a set of windows most frequently used (for normalized window range from 1 to -1):

- Bartlett: $\max(1 - |t|, 0)$
- Blackman: $0.42 + 0.5\cos(\pi t) + 0.08\cos(2\pi t)$
- Hamming: $0.54 + 0.46\cos(\pi t)$
- boxcar: $\begin{cases} 1, & \text{if } |t| \le 1 \\ 0, & \text{otherwise} \end{cases}$

In fact, they can be approximated accurately enough by one of the Kaiser windows with the corresponding β parameters:

$$\omega_\beta(t) = I_0\left(\beta\sqrt{1-t^2}\right)/I_0(\beta) \tag{9}$$

where I_0 is zeroth-order Infeld function (also called modified Bessel function). The higher the β, the narrower is the window. The comparison between the classical windows and Kaiser ones is shown on Fig. 20, the correspondence between the window and representation (9) is shown in the Table 1.

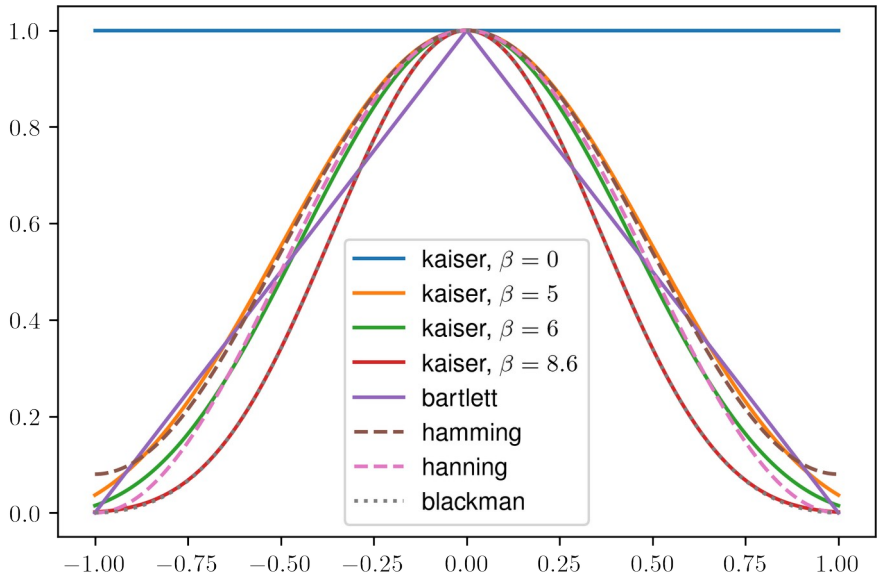

Figure 20 - Different spectral windows
DOI: https://doi.org/10.60797/COMP.2026.9.2.20

Table 1 - The correspondence between classical window types and parametric Kaiser ones

DOI: https://doi.org/10.60797/COMP.2026.9.2.21

Window	Similar to, β
boxcar	0
Hamming	5
Hanning	6
Blackman	8.6

The main consequence of the window using is the reduction of the "background" (the intervals between the peaks) and the revealing of the minor peaks, as shown on Fig. 21. This property is useful when one calculates the ratio between different spectral components; also, the narrow windows eliminate the smooth transition between peak and background, allowing to determine easily the borders of the peak. Note that the background level for Kaiser with high β is $\sim 10^{-16}$ which is about machine zero. This means that the further resolution increase is senseless.

The other side of the coin is peaks widening, that may affect the minor peaks resolution when triadic resonance instability subharmonics are studied [4]; however, since the high-frequency part of the spectrum is considered more frequently [3], [21], [22], [27], the narrow Kaiser windows for such spectral investigations are preferable.

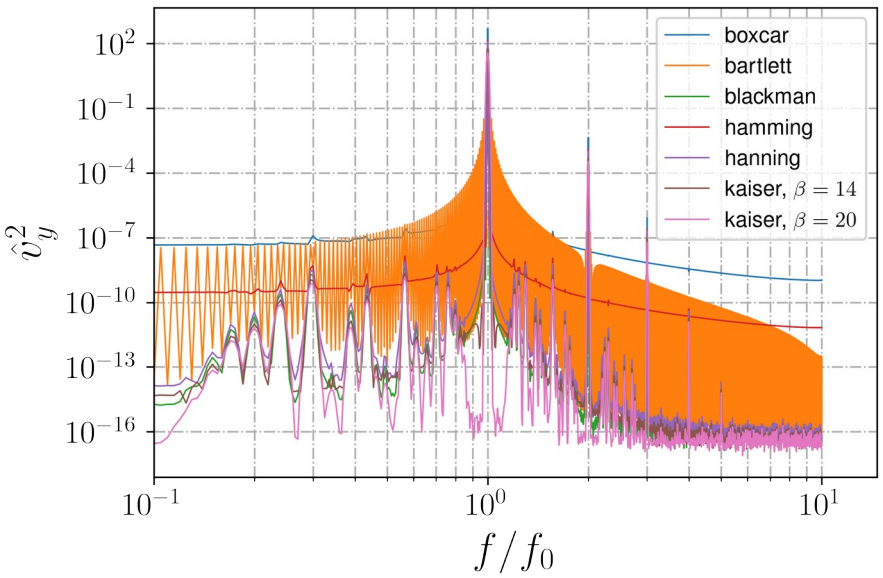

Figure 21 - Wave attractor spectrum calculated using different windows
DOI: https://doi.org/10.60797/COMP.2026.9.2.22

Despite the ability to reveal minor spectral peaks, window filtration should be applied with care. It should be always remembered that the spectral peaks after the windowing will be widened. As an example, let us consider an attractor in the two-layered fluid [22] (see shape on Fig. 22). Double spatial Fourier transform represents $f_x - f_y$ spectrogram ($f_{x,y}$ are spatial spectral numbers). As the transform is done for the whole domain, it reflexes two principle wave vector directions (for each layer of stratification, or for each attractor ray inclination angle on Fig. 22). The diagram made with no window represents these two wave directions (Fig. 23); for the windowing, the wider is the window, the worse are these directions distinguishable (Fig. 24 and 25). This occurs due to spectral peaks widening which can lead to the fatal consequences in case of double (spatial) transform. Thus, for the spatial spectra, the widest window is recommended unlike the temporal spectrum.

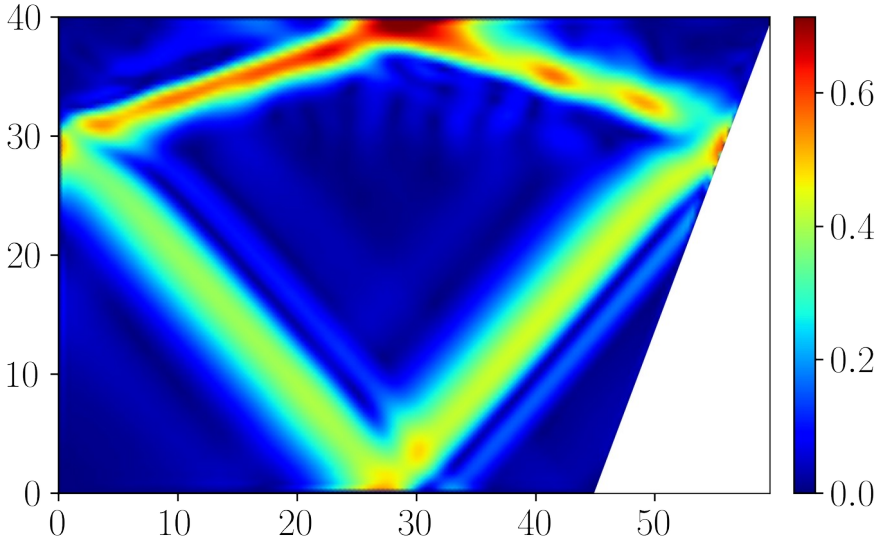

Figure 22 - Wave attractor in two-layered stratification (v_y Hilbert transform, cm/s)
DOI: https://doi.org/10.60797/COMP.2026.9.2.23

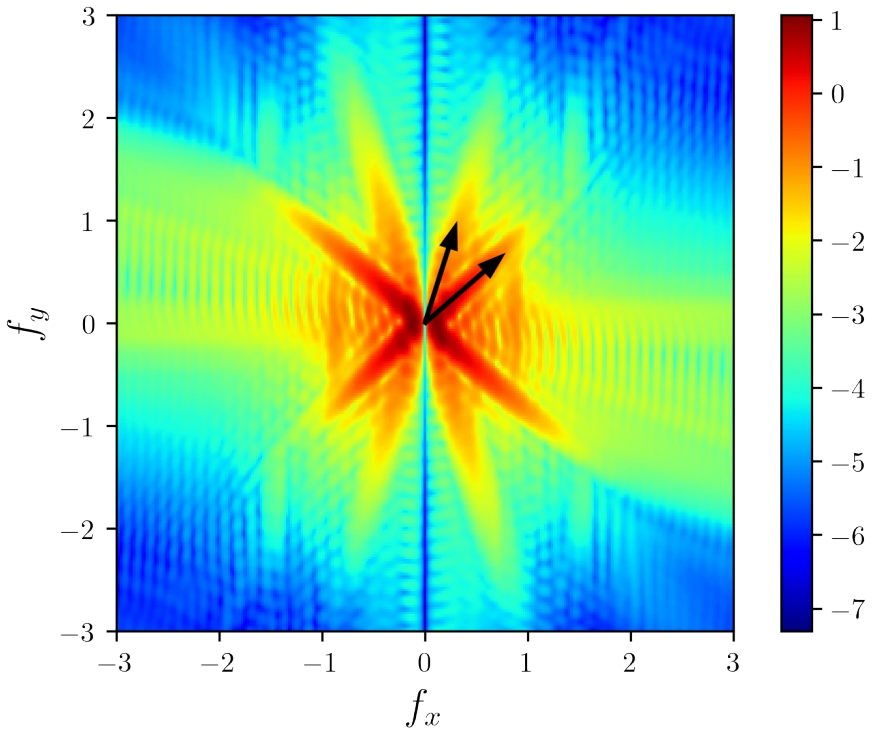

Figure 23 - f_x-f_y diagram in two-layered stratification, no window
DOI: https://doi.org/10.60797/COMP.2026.9.2.24

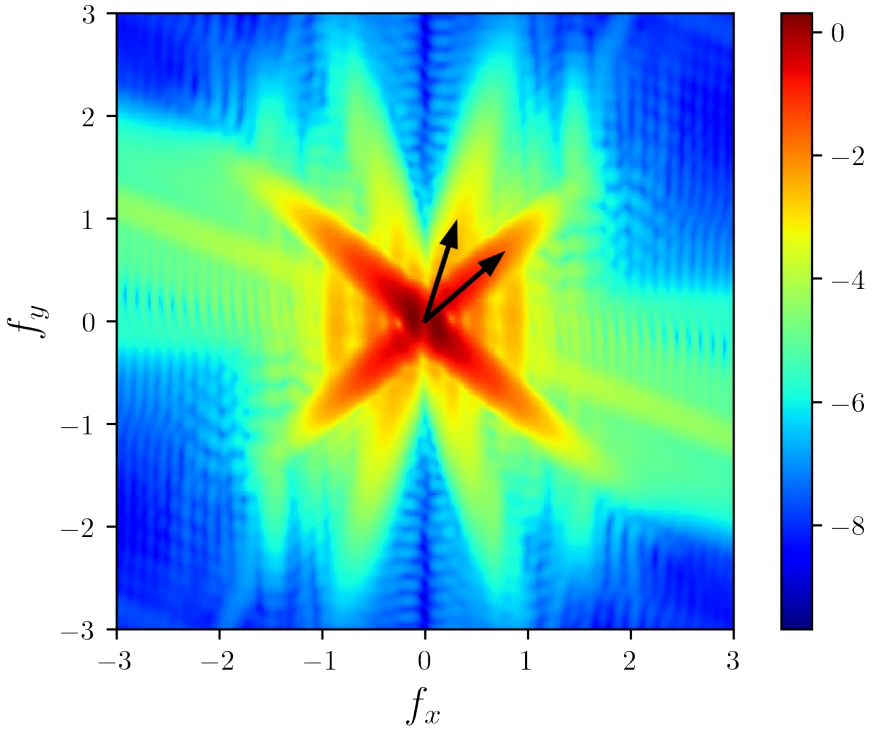

Figure 24 - f_x-f_y diagram in two-layered stratification, Kaiser window with β=5

DOI: https://doi.org/10.60797/COMP.2026.9.2.25

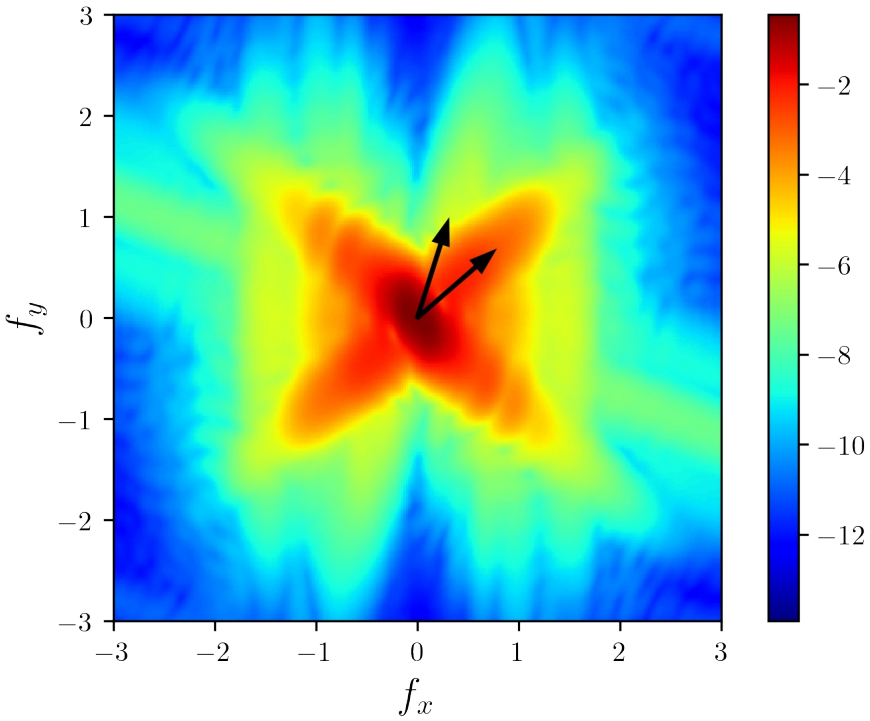

Figure 25 - f_x-f_y diagram in two-layered stratification, Kaiser window with β=14

DOI: https://doi.org/10.60797/COMP.2026.9.2.26

3.4. Colormap Selection

Wave attractor flows are known to have a specific form of the coherent structure, which is frequently considered as a marker of a wave attractor presence, and one strives to visualize it [26], [28], [30], [31]. The visualization is most frequently done by field map plotting a certain value (whether it velocity component, pressure gradient or Hilbert transform amplitude). The visualization of an attractor is a challenge [4], [26], [28]; thus, the choice of the colormap itself becomes important. The previous investigation seems to have used the colormap provided defaultly by the instrument they use: works [4], [26], [27], [31] uses "jet" colormap from *matplotlib.pyplot* package, investigations [3], [32] provides "hot" colormap preset in *VisIt* software [33], article [34] plots field maps with "inferno", [35] includes "bwr" and "hot", [29] prefers "fusion". As one can see, there is no unity in the question of the colormap selection; neither there exists a work discussing this problem.

The different visualizations are represented on Fig. 26; the plotted is the momentary velocity amplitude. The colormap labels are the same as in the *matplotlib* package [36]. For the structure emphasizing (which is most required task), "seismic" or "hot" will be the preferable option. For the background waves resolution, "turbo" is optimal. The "jet" pattern will be a good compromise between them. The other colormaps plot the attractor neither bright nor detailed.

The discrete (quantitative) colormaps can also be used for a wave-attractor visualization (Fig. 27). These ones, however, represent the background instability very poorly, which nevertheless may be useful for the structure visualization. "Accent" seems to be better for the structure emphasizing, and none of them reveal the background waves.

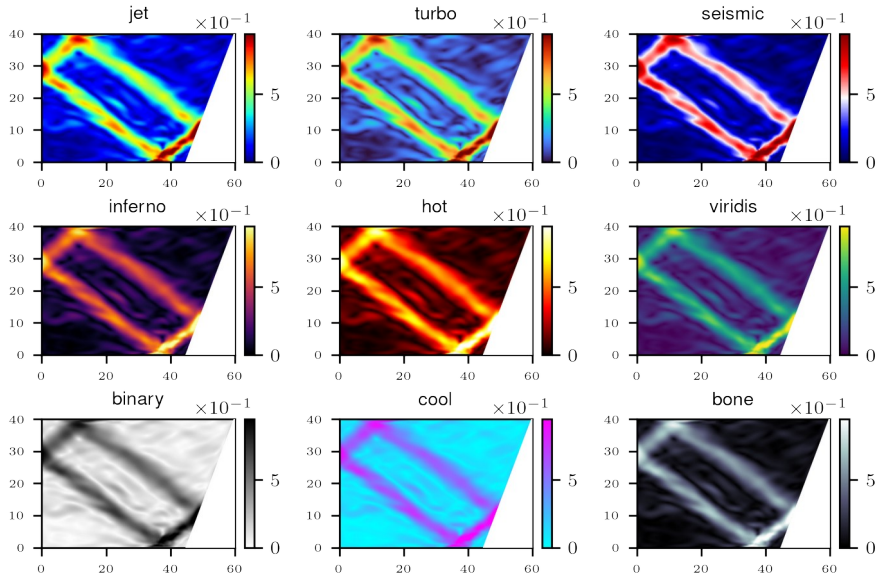

Figure 26 - A wave-attractor in a weakly-nonlinear regime visualization (|v|, cm/s): continuous colormaps
DOI: https://doi.org/10.60797/COMP.2026.9.2.27

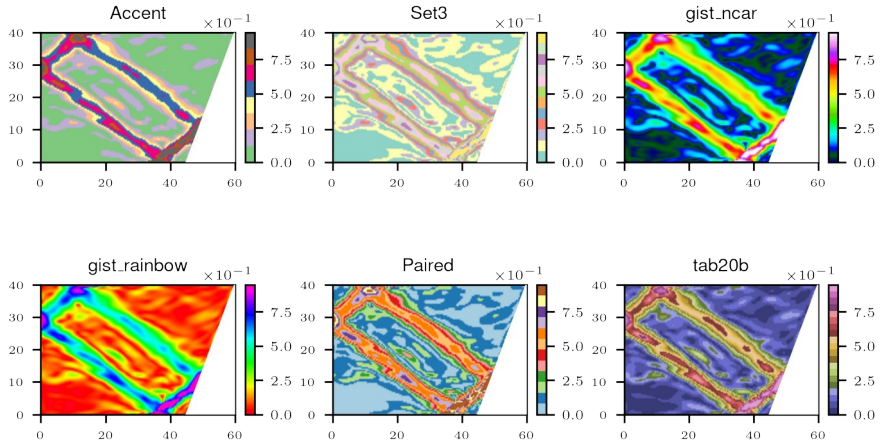

Figure 27 - A wave-attractor in a weakly-nonlinear regime visualization (|v|, cm/s): discrete colormaps
DOI: https://doi.org/10.60797/COMP.2026.9.2.28

Conclusion

Wave attractors as complex flows require a thorough selection of the methods for their processing. In this article, a number of methods were discussed. For the energy mean calculation, the best method was found that is stable for the sharp initial increase as well as for developed instability oscillations. For the spectra, different windows application were discussed and revealed that different windows should be used for spatial and temporal spectra; the influence of the spectrum spatial position is investigated for the different setups, found that it is minimal. Additionally, the field map representation is discussed, the different colormaps are applied, their aspects are shown for the selection in further works.

Конфликт интересов

Не указан.

Рецензия

Все статьи проходят рецензирование. Но рецензент или автор статьи предпочли не публиковать рецензию к этой статье в открытом доступе. Рецензия может быть предоставлена компетентным органам по запросу.

Conflict of Interest

None declared.

Review

All articles are peer-reviewed. But the reviewer or the author of the article chose not to publish a review of this article in the public domain. The review can be provided to the competent authorities upon request.

Список литературы / References

1. Maas L. Geometric focusing of internal waves / L. Maas, F.-P.A. Lam // Journal of Fluid Mechanics. — 1995. — № 300. — P. 1–41.
2. Brouzet C. Energy cascade in internal wave attractors / C. Brouzet, E. Ermanyuk, I. Sibgatullin et al. // EPL. — 2016. — № 113 (4).
3. Елистратов С. Моделирование аккумуляции кинетической энергии внутренних волн в областях с большим отношением горизонтального и вертикального масштабов / С. Елистратов, К. Ватутин, И. Сибгатуллин и др. // Труды ИСП РАН. — 2020. — № 32 (6).
4. Scolan H. Nonlinear fate of internal wave attractors / H. Scolan, E. Ermanyuk, T. Dauxois // Physical review letters. — 2013. — № 110 (23).
5. Brouzet C. Internal wave attractors: different scenarios of instability / C. Brouzet, E. Ermanyuk, S. Joubaud et al. // Journal of Fluid Mechanics. — 2017. — № 811.
6. Grisouard N. Numerical simulation of a two-dimensional internal wave attractor / N. Grisouard, C. Staquet, I. Pairaud // Journal of Fluid Mechanics. — 2008. — № 614.
7. Brouzet C. Direct numerical simulation of internal gravity wave attractor in trapezoidal domain with oscillating vertical wall / C. Brouzet, T. Dauxois, E. Ermanyuk et al. // Proceedings of the Institute for System Programming of the RAS. — 2014. — № 26 (5).
8. Jouve L. Direct numerical simulations of an inertial wave attractor in linear and nonlinear regimes / L. Jouve, G.I. Ogilvie // Journal of Fluid Mechanics. — 2014. — № 745.
9. Sibgatullin I. Direct numerical simulation of attractors of internal gravity waves and their instability in stratied fluids / I. Sibgatullin, E. Ermanyuk, C. Brouzet et al. // International Summer Course and Workshop on Complex Environmental Turbulent Flows; — Barcelona: CIMNE, 2015.
10. Brouzet C. Internal wave aractors examined using laboratory experiments and 3d numerical simulations / C. Brouzet, I. Sibgatullin, H. Scolan et al. // Journal of Fluid Mechanics. — 2016. — № 793.
11. Hazewinkel J. Comparison of laboratory and numerically observed scalar fields of an internal wave attractors / J. Hazewinkel, N. Grisouard, S. Dalziel // European Journal of Mechanics-B/Fluids. — 2011. — № 30 (1)+.
12. NEK — fast high-order scalable CFD. — URL: https://nek5000.mcs.anl.gov/ (accessed: 06.11.2025)
13. Sibgatullin I. Direct numerical simulation of three-dimensional inertial wave attractors / I. Sibgatullin, E. Ermanyuk, L. Maas et al. // 2017 Ivannikov ISPRAS Open Conference (ISPRAS) Proceedings. — 2017. — № 1.
14. Ryazanov D. About the quasihydrodynamic approach for simulation of internal wave attractors / D. Ryazanov // Mathematical modelling. — 2021. — № 23 (12).
15. Shmakova N. The power of internal wave attractors / N. Shmakova, Z. Makridin, Y. Rudaya et al. // Physics of Fluids. — 2025. — № 37.
16. Gostiaux L. A novel internal waves generator / L. Gostiaux, H. Didelle, S. Mercier et al. // Experiments in Fluids. — 2007. — № 42.
17. Mercier M. New wave generation / M. Mercier, D. Martinand, M. Mathur et al. // Journal of Fluid Mechanics. — 2010. — № 657.
18. Mercier M. Analyzing emission, reection and diraction of internal waves using the Hilbert transform / M. Mercier, N. Garnier, T. Dauxois // Annual Meeting of the APS Division of Fluid Dynamics. — 2009. — № 53.
19. Ryazanov D. Biharmonic aractors of internal gravity waves / D. Ryazanov, M. Providukhina, I. Sibgatullin et al. // Fluid Dynamics. — 2021. — № 56 (3).
20. Sibgatullin I. Internal and inertial wave aractors: A review / I. Sibgatullin, E. Ermanyuk // Journal of Applied Mechanics and Technical Physics. — 2019. — № 60 (2).
21. Elistratov S. Inuence of wave-maker shape on the wave attractor / S. Elistratov, D. Ilina // Pramana -Journal of Physics. — 2025. — № 99 (69).
22. Elistratov S. Towards the salinity prole inuence on an internal wave aractor formation / S. Elistratov, I. But // Water waves. — 2024. — № 6.
23. Huang N.E. The empirical mode decomposition and the hilbert spectrum for nonlinear and nonstationary time series analysis / N.E. Huang, Z. Shen, S.R. Long et al. // Proceedings of the Royal Society of London. — 1998. — № A 454.
24. Елистратов С.А. Пространственное POD-разложениеэпидемиологических данных COVID-19 / С.А. Елистратов // Труды ИСП РАН. — 2024. — № 36 (13).
25. Maas L. Wave aractors: linear yet nonlinear / L. Maas // International Journal of Bifurcation and Chaos. — 2003. — № 15 (09).
26. Elistratov S.A. Halocline internal wave aractors visualization / S.A. Elistratov // Scientic visualization. — 2024. — № 16 (1).
27. Elistratov S. Wave attractor in basin with underwater step: from discrete to continuous energy spectrum / S. Elistratov, I. But // Indian Journal of Physics. — 2025. — № 99.
28. Ryazanov D. Visualisation for ows with internal waves attractor / D. Ryazanov, S. Elistratov, M. Kraposhin // Scientific Visualization. — 2021. — № 13 (5).
29. van Oers M. In situ measurement of wave attractor induced forces / M. van Oers, L.R.M. Maas // Experiments in Fluids. — 2022. — № 63 (12).
30. Elistratov S. POD-based hydrodynamical structures visualization in ows with an internal wave attractor / S. Elistratov // Scientific Visualization. — 2023. — № 15 (2).
31. Elistratov S. On the visualization of subatractor under mixed tidal forcing / S. Elistratov // Scientific Vizualization. — 2022. — № 17.

32. Sibgatullin I. On (n,1) wave attractors: Coordinates and saturation time / I. Sibgatullin, A. Petrov, L. Maas et al. // Symmetry. — 2022. — № 14 (2).

33. VisIt Home. — URL: https://visit-dav.github.io/visit-website/index.html (accessed: 06.11.2025)

34. Bajars J. On the appearance of internal wave attractors due to an initial or parametrically excited disturbance / J. Bajars, J Frank, L.R.M. Maas // Journal of Fluid Mechanics. — 2017. — № 714.

35. Maas L.R.M. Observation of an internal wave attractor in a conned, stably stratied fluid / L.R.M. Maas, D. Benielli, J. Sommeria et al. // Nature. — 1997. — № 388.

36. Matplotlib: Visualization with Python. — URL: https://matplotlib.org/ (accessed: 06.11.2025)

Список литературы на английском языке / References in English

1. Maas L. Geometric focusing of internal waves / L. Maas, F.-P.A. Lam // Journal of Fluid Mechanics. — 1995. — № 300. — P. 1–41.

2. Brouzet C. Energy cascade in internal wave attractors / C. Brouzet, E. Ermanyuk, I. Sibgatullin et al. // EPL. — 2016. — № 113 (4).

3. Elistratov S. Modelirovanie akkumulyacii kineticheskoj e'nergii vnutrennix voln v oblastyax s bol'shim otnosheniem gorizontal'nogo i vertikal'nogo masshtabov [Numerical simulation of internal waves and effects of accumulation of kinetic energy in large aspect ratio domains] / S. Elistratov, K. Vatutin, I. Sibgatullin et al. // Proceedings of ISP RAS. — 2020. — № 32 (6). [in Russian]

4. Scolan H. Nonlinear fate of internal wave attractors / H. Scolan, E. Ermanyuk, T. Dauxois // Physical review letters. — 2013. — № 110 (23).

5. Brouzet C. Internal wave attractors: different scenarios of instability / C. Brouzet, E. Ermanyuk, S. Joubaud et al. // Journal of Fluid Mechanics. — 2017. — № 811.

6. Grisouard N. Numerical simulation of a two-dimensional internal wave attractor / N. Grisouard, C. Staquet, I. Pairaud // Journal of Fluid Mechanics. — 2008. — № 614.

7. Brouzet C. Direct numerical simulation of internal gravity wave attractor in trapezoidal domain with oscillating vertical wall / C. Brouzet, T. Dauxois, E. Ermanyuk et al. // Proceedings of the Institute for System Programming of the RAS. — 2014. — № 26 (5).

8. Jouve L. Direct numerical simulations of an inertial wave attractor in linear and nonlinear regimes / L. Jouve, G.I. Ogilvie // Journal of Fluid Mechanics. — 2014. — № 745.

9. Sibgatullin I. Direct numerical simulation of attractors of internal gravity waves and their instability in stratied fluids / I. Sibgatullin, E. Ermanyuk, C. Brouzet et al. // International Summer Course and Workshop on Complex Environmental Turbulent Flows; — Barcelona: CIMNE, 2015.

10. Brouzet C. Internal wave aractors examined using laboratory experiments and 3d numerical simulations / C. Brouzet, I. Sibgatullin, H. Scolan et al. // Journal of Fluid Mechanics. — 2016. — № 793.

11. Hazewinkel J. Comparison of laboratory and numerically observed scalar fields of an internal wave attractors / J. Hazewinkel, N. Grisouard, S. Dalziel // European Journal of Mechanics-B/Fluids. — 2011. — № 30 (1)+.

12. NEK — fast high-order scalable CFD. — URL: https://nek5000.mcs.anl.gov/ (accessed: 06.11.2025)

13. Sibgatullin I. Direct numerical simulation of three-dimensional inertial wave attractors / I. Sibgatullin, E. Ermanyuk, L. Maas et al. // 2017 Ivannikov ISPRAS Open Conference (ISPRAS) Proceedings. — 2017. — № 1.

14. Ryazanov D. About the quasihydrodynamic approach for simulation of internal wave attractors / D. Ryazanov // Mathematical modelling. — 2021. — № 23 (12).

15. Shmakova N. The power of internal wave attractors / N. Shmakova, Z. Makridin, Y. Rudaya et al. // Physics of Fluids. — 2025. — № 37.

16. Gostiaux L. A novel internal waves generator / L. Gostiaux, H. Didelle, S. Mercier et al. // Experiments in Fluids. — 2007. — № 42.

17. Mercier M. New wave generation / M. Mercier, D. Martinand, M. Mathur et al. // Journal of Fluid Mechanics. — 2010. — № 657.

18. Mercier M. Analyzing emission, reection and diraction of internal waves using the Hilbert transform / M. Mercier, N. Garnier, T. Dauxois // Annual Meeting of the APS Division of Fluid Dynamics. — 2009. — № 53.

19. Ryazanov D. Biharmonic aractors of internal gravity waves / D. Ryazanov, M. Providukhina, I. Sibgatullin et al. // Fluid Dynamics. — 2021. — № 56 (3).

20. Sibgatullin I. Internal and inertial wave aractors: A review / I. Sibgatullin, E. Ermanyuk // Journal of Applied Mechanics and Technical Physics. — 2019. — № 60 (2).

21. Elistratov S. Inuence of wave-maker shape on the wave attractor / S. Elistratov, D. Ilina // Pramana -Journal of Physics. — 2025. — № 99 (69).

22. Elistratov S. Towards the salinity prole inuence on an internal wave aractor formation / S. Elistratov, I. But // Water waves. — 2024. — № 6.

23. Huang N.E. The empirical mode decomposition and the hilbert spectrum for nonlinear and nonstationary time series analysis / N.E. Huang, Z. Shen, S.R. Long et al. // Proceedings of the Royal Society of London. — 1998. — № A 454.

24. Elistratov S.A. Prostranstvennoe POD-razlozheniee'pidemiologicheskix danny'x COVID-19 [COVID-19 Epidemiological Indicators POD Spatial Decomposition] / S.A. Elistratov // Proceedings of the Institute for System Programming of the RAS. — 2024. — № 36 (13). [in Russian]

25. Maas L. Wave aractors: linear yet nonlinear / L. Maas // International Journal of Bifurcation and Chaos. — 2003. — № 15 (09).

26. Elistratov S.A. Halocline internal wave aractors visualization / S.A. Elistratov // Scientic visualization. — 2024. — № 16 (1).

27. Elistratov S. Wave attractor in basin with underwater step: from discrete to continuous energy spectrum / S. Elistratov, I. But // Indian Journal of Physics. — 2025. — № 99.

28. Ryazanov D. Visualisation for ows with internal waves attractor / D. Ryazanov, S. Elistratov, M. Kraposhin // Scientific Visualization. — 2021. — № 13 (5).

29. van Oers M. In situ measurement of wave attractor induced forces / M. van Oers, L.R.M. Maas // Experiments in Fluids. — 2022. — № 63 (12).

30. Elistratov S. POD-based hydrodynamical structures visualization in ows with an internal wave attractor / S. Elistratov // Scientific Visualization. — 2023. — № 15 (2).

31. Elistratov S. On the visualization of subatractor under mixed tidal forcing / S. Elistratov // Scientific Vizualization. — 2022. — № 17.

32. Sibgatullin I. On (n,1) wave attractors: Coordinates and saturation time / I. Sibgatullin, A. Petrov, L. Maas et al. // Symmetry. — 2022. — № 14 (2).

33. VisIt Home. — URL: https://visit-dav.github.io/visit-website/index.html (accessed: 06.11.2025)

34. Bajars J. On the appearance of internal wave attractors due to an initial or parametrically excited disturbance / J. Bajars, J Frank, L.R.M. Maas // Journal of Fluid Mechanics. — 2017. — № 714.

35. Maas L.R.M. Observation of an internal wave attractor in a conned, stably stratied fluid / L.R.M. Maas, D. Benielli, J. Sommeria et al. // Nature. — 1997. — № 388.

36. Matplotlib: Visualization with Python. — URL: https://matplotlib.org/ (accessed: 06.11.2025)